# Confronting Color Dipole and Intrinsic $k_T$ Approaches in D–Y Dilepton Production

Marcos André Betemps
*Conjunto Agrotécnico Visconde da Graça,*
*Universidade Federal de Pelotas,*
*Caixa Postal 460, 96060-290 Pelotas,*
*Rio Grande do Sul, Brazil*
*E-mail: marcos.betemps@ufpel.edu.br*

Maria Beatriz Gay Ducati, and Emmanuel Gräve de Oliveira
*Instituto de Física,*
*Universidade Federal do Rio Grande do Sul,*
*Caixa Postal 15051, 91501-970 Porto Alegre,*
*Rio Grande do Sul, Brazil*
*E-mail: beatriz.gay@ufrgs.br,*
*E-mail: emmanuel.deoliveira@ufrgs.br*

(Received on 10 July, 2008)

We study the Drell-Yan dilepton production in proton-nucleus collisions at RHIC energies. We use two different approaches: the usual intrinsic transverse momentum approach at NLO in the infinitum momentum frame; and the color dipole in the target rest frame. We compare both formalisms at backward rapidities (proton as a target). At forward rapidities, we use earlier results considering the nucleus in a Color Glass Condensate phase. We show qualitative agreement between the two formalisms through the nuclear modification ratio as a function of both rapidity and transverse momentum and that low-mass dileptons are relevant observables to probe nuclear effects.

Keywords: Drell-Yan process; Dilepton production; Nuclear effects; Dipole frame; Infinite momentum frame

In a recent work[1], Drell-Yan dilepton production at backward rapidities in hadrons collisions was studied in the rest frame of the target, i. e., in the color dipole approach. In this work, we compare these previous results with results obtained used well know intrinsic $k_T$ approach in the infinitum momentum frame [2, 3]. In this frame, the process is understood as the combination of two partons to create a virtual boson that subsequently splits in the dilepton. For dilepton mass $M$ much smaller than the Z mass, the dominant process includes only the photon as the virtual boson. The dilepton production is of particular interest since dileptons do not interact strongly and therefore carry information about initial state effects.

The kinematics used here are described now. Partons and hadrons are taken as massless, the momenta of hadrons $A$ and $B$ are $P_A$ and $P_B$, and the momenta of partons are $p_A = x_A P_A$ and $p_B = x_B P_B$ (for now, partons are collinear to hadrons). The virtual photon momentum is $q$ and $q^2 = M^2$ is the squared dilepton mass. The Mandelstam variables are given by: $s = 2P_A \cdot P_B$, $t = (q - P_A)^2$, and $u = (q - P_B)^2$. We also define $x_1 = 2P_B \cdot q/s$, $x_2 = 2P_A \cdot q/s$, and the photon rapidity $y = \frac{1}{2}\ln(x_1/x_2)$. It can be showed that:

$$x_{1,2} = \sqrt{\frac{M^2 + p_T^2}{s}} \mathrm{e}^{\pm y}, \tag{1}$$

in which $p_T$ is the photon (also dilepton) transverse momentum.

In IMF collinear approximation, partons are considered collinear to hadrons, without intrinsic transverse momentum. Using this framework at leading order, experimental results of transverse momentum distribution cannot be reproduced: although valid for large $p_T$, collinear NLO $p_T$ distribution diverges at $p_T = 0$ and is not in agreement with experiments for small $p_T$. We consider then partonic intrinsic transverse momentum, i. e., partons are not collinear to hadrons [2, 3]. The partonic distributions are change as the following prescription:

$$f(x)dx \to f(x)h(\vec{k_T})dxd^2k_T. \tag{2}$$

In this paper, we consider $h(\vec{k_T}) = \frac{1}{2\pi b^2}\exp\left(\frac{k_T^2}{2b^2}\right)$. Therefore, the cross section is given by[4, 5]:

$$\sigma_S(s, M^2, y, p_T) = h'(p_T^2)\frac{d\sigma}{dM^2 dy} + \int d^2q_T \sigma_P(s, M^2, q_T^2)[h'((\vec{p}_T - \vec{q}_T)^2) - h'(p_T^2)]. \tag{3}$$

In the above expression, it is included the NLO collinear double differential cross section:

$$\begin{aligned}\frac{d\sigma}{dM^2 dy} &= \frac{\hat{\sigma}_0}{s}\int_0^1 dx_A dx_B dz \delta(x_A x_B z - \tau)\delta\left(y - \frac{1}{2}\ln\frac{x_A}{x_B}\right) \\ &\times \left\{P_{q\bar{q}}(x_A, x_B, M^2)\left[\delta(1-z) + \frac{\alpha_s(M^2)}{2\pi}D_q(z)\right]\right. \\ &+ \left. P_{qg+gq}(x_A, x_B, M^2)\left[\frac{\alpha_s(M^2)}{2\pi}D_g(z)\right]\right\}.\end{aligned}$$

Using the modified minimal subtraction scheme ($\overline{\mathrm{MS}}$), $D_q(z)$ and $D_g(z)$ are given e.g. in Ref. [6] ($C_F = 4/3$, $T_R = 1/2$).

The second term in the right hand side of equation 3 is calculated only from annihilation and Compton diagrams and is written as[5]:

$$\sigma_P(s,M^2,p_T^2) = \frac{1}{\pi^2}\frac{\alpha^2\alpha_s}{M^2\hat{s}^2}\int_{x_{A\min}}^1 dx_A \frac{x_B x_A}{x_A - x_1}\left\{P_{q\bar{q}}(x_A,x_B,M^2)\frac{8}{27}\frac{2M^2\hat{s}+\hat{u}^2+\hat{t}^2}{\hat{t}\hat{u}}\right.$$
$$\left. + P_{qg}(x_A,x_B,M^2)\frac{1}{9}\frac{2M^2\hat{u}+\hat{s}^2+\hat{t}^2}{-\hat{s}\hat{t}} + P_{gq}(x_A,x_B,M^2)\frac{1}{9}\frac{2M^2\hat{t}+\hat{s}^2+\hat{u}^2}{-\hat{s}\hat{u}}\right\}$$

in which $x_{A\min}$ is given by $(x_1-\tau)/(1-x_2)$, $x_B = (x_A x_2 - \tau)/(x_a - x_1)$, and

$$P_{q\bar{q}}(x_A,x_B) = \sum_q e_q^2\,(f_q(x_A)f_{\bar{q}}(x_B) + \bar{q}\leftrightarrow q) \quad (4)$$

$$P_{qg}(x_A,x_B) = \sum_q e_q^2\,(f_q(x_A) + f_{\bar{q}}(x_A))\,f_g(x_B) \quad (5)$$

$$P_{gq}(x_A,x_B) = \sum_q e_q^2 f_g(x_A)\,(f_q(x_B) + f_{\bar{q}}(x_B))\,. \quad (6)$$

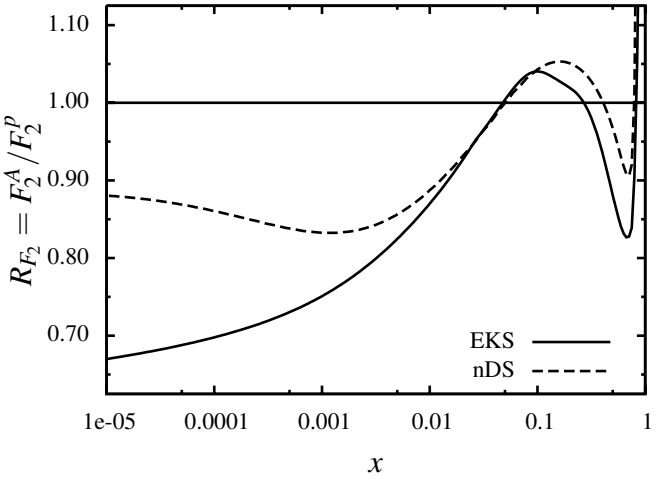


FIG. 1: Ratio $R_{F_2}^A = F_2^A/F_2^p$ using EKS and nDS parameterizations.

In the color dipole approach, Drell–Yan dilepton production is studied in the rest frame of the target. Diagrams considered now look like projectile quark *bremsstrahlung* on the target color field. So, the projectile emits a quark (or antiquark), this parton fluctuates in a state of quark–photon and interacts with the color field of the target, and the photon is freed to split in a dilepton. The color dipole cross section arises as interference of the diagram in which the quark first interacts with the target with the diagram in which the quark first fluctuates in the quark–photon state. This result was first stated in [7] and derived in detail in [4].

In [1], the color dipole approach was used to study dileptons produced at backward rapidities, so the proton was considered as the target and the nucleus as the projectile. In this case, the color dipole approach is phenomenologically valid for small $x_1$[4] – very backward rapidities. The cross section is written as:

$$\frac{d\sigma^{DY}}{dM^2 dy d^2p_T} = \frac{\alpha_{em}^2}{6\pi^3 M^2}\int_0^\infty d\rho W(x_2,\rho,p_T)\sigma_{\rm dip}(x_1,\rho), \quad (7)$$

in which $\rho$ is the dipole transverse size. In this case, $x_2$ is the projectile momentum fraction carried by the virtual photon.

The weight function $W(x_2,\rho,p_T)$ contains the nuclear structure function $F_2^A(x_2/\alpha,M^2) = \sum_q e_q^2[x f_q^A(x,M^2) + x f_{\bar{q}}^A(x,M^2)]$:

$$W(x_2,\rho,p_T) = \int_{x_2}^1 \frac{d\alpha}{\alpha^2}F_2^A(\frac{x_2}{\alpha},M^2)\left\{[m_q^2\alpha^4 + 2M^2(1-\alpha)^2]\left[\frac{1}{p_T^2+\eta^2}T_1(\rho) - \frac{1}{4\eta}T_2(\rho)\right]\right.$$
$$\left. + \;[1+(1-\alpha)^2]\left[\frac{\eta p_T}{p_T^2+\eta^2}T_3(\rho) - \frac{1}{2}T_1(\rho) + \frac{\eta}{4}T_2(\rho)\right]\right\},$$

in which $\eta^2 = (1-\alpha)M^2 + \alpha^2 m_q^2$ and $m_q = 0,2$ GeV is the quark mass. The functions $T_i$ are given by:

$$T_1(\rho) = \frac{\rho}{\alpha}J_0\left(\frac{p_T\rho}{\alpha}\right)K_0\left(\frac{\eta\rho}{\alpha}\right) \quad (8)$$

$$T_2(\rho) = \frac{\rho^2}{\alpha^2}J_0\left(\frac{p_T\rho}{\alpha}\right)K_1\left(\frac{\eta\rho}{\alpha}\right) \quad (9)$$

$$T_3(\rho) = \frac{\rho}{\alpha}J_1\left(\frac{p_T\rho}{\alpha}\right)K_1\left(\frac{\eta\rho}{\alpha}\right), \quad (10)$$

in which $J_n(x)$ is the Bessel function of first kind and $K_n(x)$ is the modified Bessel function of second kind.

We use the model introduced by Golec-Biernat e Wüsthoff (GBW)[8] for the dipole cross section:

$$\sigma_{dip}(x,r) = \sigma_0\left[1 - \exp\left(-\frac{r^2Q_0^2}{4(x/x_0)^\lambda}\right)\right], \quad (11)$$

in which $Q_0^2 = 1$ GeV$^2$ and there are three fitted parameters: $\sigma_0 = 23,03$ mb (59,14 GeV$^{-2}$), $x_0 = 3,04\times10^{-4}$, and $\lambda =$

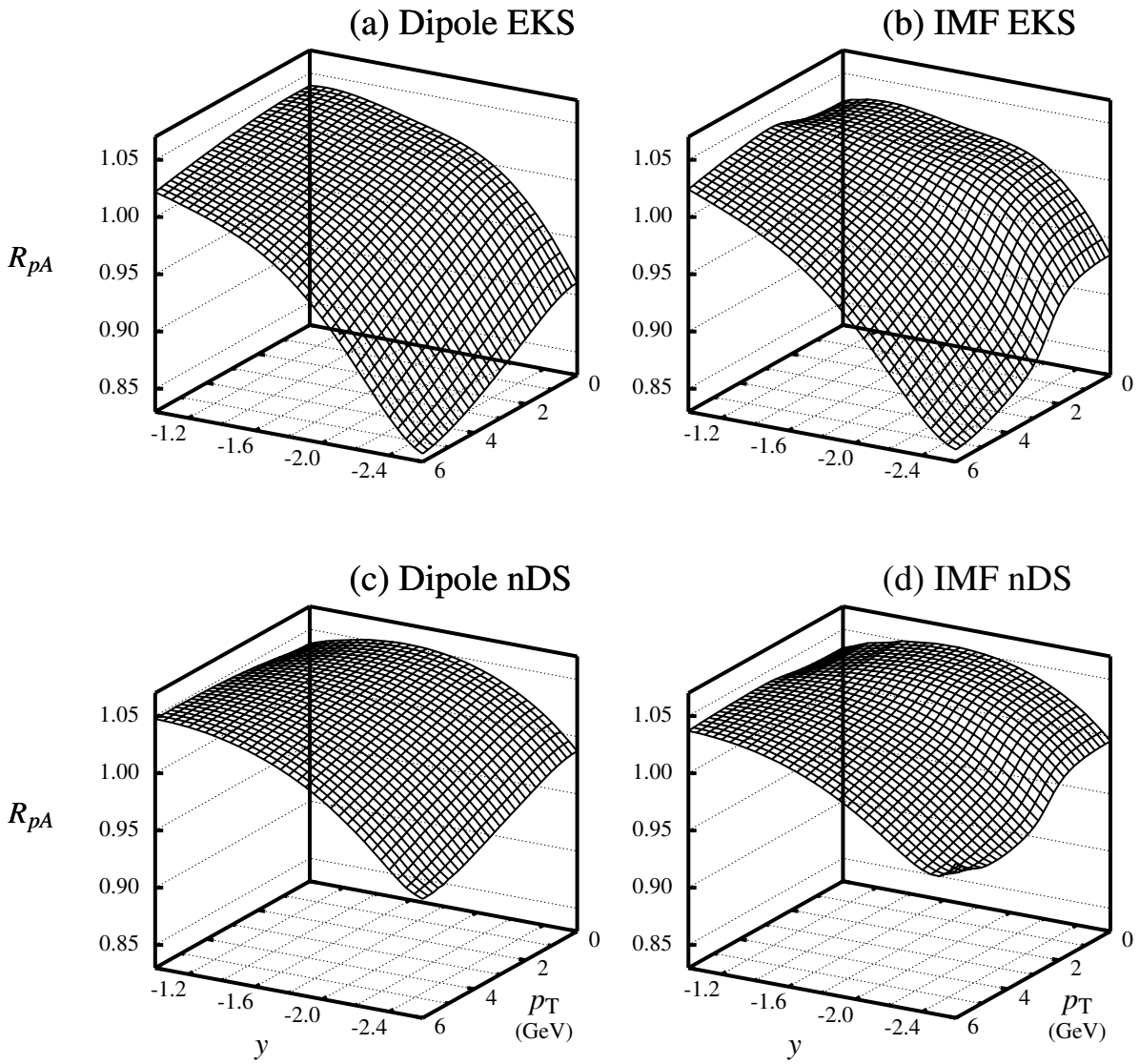


FIG. 2: Factor $R_{pA}$ at RHIC energies as a function of rapidity and transverse momentum.

0, 288. It is important to highlight that the present dipole cross section includes saturation effects, not included in the IMF approach.

We use GRV98[9, 10] as the parton distribution function (PDF) of free protons. Two parameterizations of the nuclear PDFs are used: EKS[11–13] and nDS[14]. EKS parameterization gives the nPDF as the free proton PDF multiplied by a factor: $f_q^A(x,Q) = R_q^A(x,Q) f_q^p(x,Q)$, while nDS gives the nPDF as a convolution of the free proton PDF and a weight function:

$$f_q^A(x,Q) = \int_x^A \frac{dy}{y} W_q(y,A) f_q^p\left(\frac{x}{y},Q\right). \qquad (12)$$

EKS parameterization is available only at leading order, while nDS is also at NLO. In Fig. 1, both parameterizations are compared at leading order calculating $R_{F_2}^A = F_2^A/F_2^p$. We would like to stress that nDS parameterization presents lower ratio for most values of $x$ studied, in particular for EMC ($0.3 < x < 0.8$) and shadowing ($x < 0.1$) effects – other regions correspond to anti-shadowing ($0.1 < x < 0.3$) and Fermi motion ($0.8 < x$) effects.

We use dilepton mass of $M = 6.5$ GeV, RHIC energies ($\sqrt{s} = 200$ GeV), gold nucleus ($A = 196.97$), and intrinsic $k_T$ standard deviation of $b = 0.48$ GeV. In Fig. 2, the nuclear modification factor:

$$R_{pA} = \frac{d\sigma(pA)}{dp_T^2 dy dM} \Big/ A\frac{d\sigma(pp)}{dp_T^2 dy dM} \qquad (13)$$

is calculated using both formalisms described earlier in the region of backward rapidity. EKS and nDS parameterizations give qualitatively similar results, showing that both approaches roughly give the same dependence of $R_{pA}$ on the nuclear effects. The main difference is a step near $p_T = 2.5$ GeV in the IMF distributions, caused by the different ways that the two terms in Eq. 3 take into account nuclear effects, since each

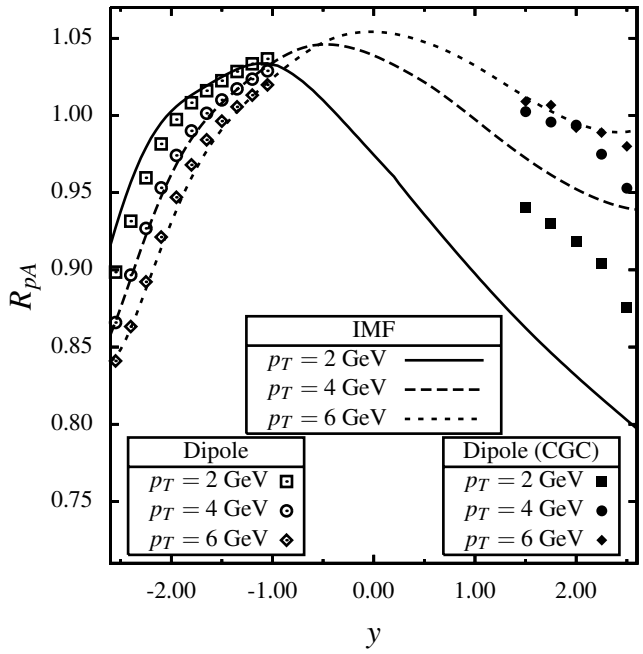


FIG. 3: Factor $R_{pA}$ calculated using three different approaches: infinite momentum frame, color dipole at backward rapidities, and color dipole at forward rapidities considering the nucleus as a CGC [15].

is dominant in one region of $p_T$. This result shows that saturation effects included in the dipole approach are not very effective in changing the nuclear modification ratio.

The behavior of $R_{pA}$ is mainly explained by the inclusion of anti-shadowing effects with decreasing $x_2$ approximately from 0.64 ($y = -2.6, p_T = 7$) to 0.09 ($y = -1.0, p_T = 0$). Anti-shadowing effects are characterized by an increase in the nuclear cross section, exactly what is seen in Fig. 2. EKS parameterization predicts a smaller $R_{pA}$ than nDS parameterization in both approaches and nDS parameterization shows more sensibility to the approach change, as it is expect, since nDS parameterization is different whether LO or NLO is considered.

In Fig. 3, we combine color dipole results obtained here at backward rapidities, color dipole results obtained in Ref. [15] at forward rapidities considering the nucleus as a CGC phase, and IMF results. EKS parameterization was used when a nuclear PDF was required. Overall, we see a qualitative agreement among the approaches and that the ratio $R_{pA}$ dependence on $p_T$ is consistently obtained: if $y < 0$ ($y > 0$), $R_{pA}$ decreases (increases) with a increase of $p_T$, thanks to the anti-shadowing (shadowing) effect.

In conclusion, we saw that low-mass dileptons are relevant in probing nuclear effects at RHIC energies. Either at backward or forward rapidities, results obtained showed strong dependence on the nuclear effects and in the choice of the parameterization. Among the approaches, qualitative agreement was obtained in the nuclear modification factor, showing that saturation effects (considered in the color dipole formalism and in the CGC) do not play a key role in this factor. However, the nuclear modification factor proved to be very sensitive to the introduction of a intrinsic transverse momentum, given the step seen in the $p_T$ distribution.


[1] M. A. Betemps, M. B. Gay Ducati, and E. G. de Oliveira, Phys. Rev. D **74**, 094010 (2006), hep-ph/0607247.

[2] G. Altarelli, G. Parisi, and R. Petronzio, Phys. Lett. B **76**, 351 (1978).

[3] G. Altarelli, G. Parisi, and R. Petronzio, Phys. Lett. B **76**, 356 (1978).

[4] J. Raufeisen, J.-C. Peng, and G. C. Nayak, Phys. Rev. D **66**, 034024 (2002), hep-ph/0204095.

[5] R. D. Field, *Applications of Perturbative QCD*, vol. 77 of *Frontiers in Physics* (Addison-Wesley, Redwood City, 1989).

[6] R. K. Ellis, W. J. Stirling, and B. R. Webber, *QCD and Collider Physics*, vol. 8 of *Camb. Monogr. Part. Phys. Nucl. Phys. Cosmol.* (Cambridge University, Cambridge, 1996).

[7] B. Kopeliovich, in *Workshop Hirschegg'95: Dynamical Properties of Hadrons in Nuclear Matter*, edited by H. Feldmeier and W. Nörenberg (GSI, Darmstadt, 1995), pp. 102–112, hep-ph/9609385.

[8] K. J. Golec-Biernat and M. Wusthoff, Phys. Rev. D **59**, 014017 (1999), hep-ph/9807513.

[9] M. Gluck, E. Reya, and A. Vogt, Eur. Phys. J. C **5**, 461 (1998), hep-ph/9806404.

[10] M. Gluck, E. Reya, and A. Vogt, Z. Phys. C **67**, 433 (1995).

[11] K. J. Eskola, V. J. Kolhinen, and P. V. Ruuskanen, Nucl. Phys. B **535**, 351 (1998), hep-ph/9802350.

[12] K. J. Eskola, V. J. Kolhinen, and C. A. Salgado, Eur. Phys. J. C **9**, 61 (1999), hep-ph/9807297.

[13] K. J. Eskola, V. J. Kolhinen, H. Paukkunen, and C. A. Salgado, JHEP **05**, 002 (2007), hep-ph/0703104.

[14] D. de Florian and R. Sassot, Phys. Rev. D **69**, 074028 (2004), hep-ph/0311227.

[15] M. A. Betemps and M. B. Gay Ducati, Phys. Rev. D **70**, 116005 (2004), hep-ph/0408097.

[16] W. J. Stirling and M. R. Whalley, J. Phys. G **19**, D1 (1993).

[17] P. L. McGaughey, J. M. Moss, and J. C. Peng, Ann. Rev. Nucl. Part. Sci. **49**, 217 (1999), hep-ph/9905409.

[18] J. Raufeisen and J.-C. Peng, Phys. Rev. D **67**, 054008 (2003), hep-ph/0211422.